Semiclassical vibrational energies and transition frequencies for a Hamiltonian with stretch–bend potential energy coupling: Application of Fourier methods

A. Garcia-Ayllon
Department of Chemistry, Baker Laboratory, Cornell University, Ithaca, New York 14853 and Departamento de Quimica-Fisica, Facultad de CC. Quimicas, Universidad Complutense, 28040 Madrid, Spain

C. C. Martens[a)]
Department of Chemistry, Baker Laboratory, Cornell University, Ithaca, New York 14853

J. Santamaria
Departamento de Quimica-Fisica, Facultad de CC. Quimicas, Universidad Complutense, 28040 Madrid, Spain

G. S. Ezra[b)]
Department of Chemistry, Baker Laboratory, Cornell University, Ithaca, New York 14853

(Received 21 May 1987; accepted 21 August 1987)

Semiclassical methods are applied to determine transition frequencies and vibrational energies for the two-mode HC_2 stretch–bend Hamiltonian recently studied by Swamy and Hase [J. Chem. Phys. **84**, 361 (1986)]. The mean action spectral approximation for calculating transition frequencies is found to give results in excellent agreement with quantum variational values. The FFT EBK method is used to calculate vibrational eigenvalues for both nonresonant and 3:1 resonant states. Both approaches give results more accurate than those reported by Swamy and Hase using the DeLeon–Heller–Miller method. The presence of stretch–bend potential coupling is found to reduce the extent of classical chaos.

I. INTRODUCTION

The spectral and dynamical consequences of Fermi resonances between CH stretches and lower frequency bending modes have been examined recently for several systems.[1–4] A 2:1 resonance between the CH bond stretch and the adjacent HCC wag has been identified as a primary mechanism for rapid CH energy relaxation in benzene, and is an essential feature of the theoretical analysis of CH overtone linewidths given by Sibert *et al.*[3] Although the classical trajectory calculations of Sibert *et al.* yield subpicosecond relaxation times in agreement with the overtone linewidths (assumed homogeneous) measured at room temperature,[5] they include only kinetic stretch–bend coupling, and neglect potential coupling. It is clear on physical grounds, however, that the CH wag force constant must be attenuated by stretching of the CH bond, and potential coupling of this type has been found in *ab initio* calculations on several species.[6] The classical trajectory simulations of Lu *et al.* have shown that the rate and nature of overtone relaxation in planar benzene depend strongly on the presence or absence of potential coupling.[7] In particular, increasing the strength of the stretch–bend coupling decreases the decay rate constant for those overtone states exhibiting exponential decay of probability, and moves the onset of nonexponential decay to lower values of n, the number of quanta initially in the CH bond. In a recent study of the stability of the periodic orbit corresponding to CH bond stretching as a function of CH excitation energy in a two-mode model fragment of benzene, it has been shown that potential coupling decreases the range of instability[8] of the CH bond, thereby suppressing overtone relaxation.[9]

In this paper we apply semiclassical methods to calculate energy levels and transition frequencies for a two-mode vibrational Hamiltonian describing the CH stretch and HCC bend motions in an HC_2 hydrocarbon fragment. The nonseparable Hamiltonian includes both kinetic and potential coupling terms. This system has been recently studied by Swamy and Hase,[10] who calculated vibrational eigenvalues and transition frequencies using two approximate semiclassical methods: the Sorbie–Handy method,[11] which involves an implicit assumption of separability in a given coordinate system,[12] and Miller's procedure,[13] which involves linear extrapolation from nonquantizing trajectories in addition to the assumption of separability (see also the related work of DeLeon and Heller[14]). Swamy and Hase compared their semiclassical eigenvalues and transition frequencies with variational quantum results, and concluded that the approximate semiclassical methods, in particular Miller's method, did not give accurate results. It was suggested that stretch–bend resonances were responsible for the poor results obtained with the semiclassical methods.[10]

The purpose of the present work is twofold. First, we show that very accurate values for transition frequencies between various stretch–bend levels of the HC_2 system studied by Swamy and Hase can be obtained using the simple spectral method due to Noid *et al.*[15–17] In this approximate method, the energy difference between two states differing by unity in the value of a single quantum number is obtained

[a)] Mathematical Sciences Institute Fellow.
[b)] Alfred P. Sloan Foundation Fellow.

 0021-9606/87/236609-09$02.10

by Fourier transforming a single trajectory run at the *mean* action (either "good" or zeroth-order[17]), in the spirit of the Heisenberg correspondence principle.[18] We show that the spectral method gives remarkably accurate transition frequencies for both nonresonant and resonant trajectories, even when zeroth-order mean actions are used. Second, we apply the recently developed EBK FFT semiclassical quantization method[19–21] to determine vibrational eigenvalues for the HC_2 system. The EBK FFT approach involves accurate calculation of good classical actions, and so provides "exact" primitive semiclassical results. The method can be applied to nonresonant[20] and resonant[21] systems. For the HC_2 Hamiltonian studied here, there are regions of classical phase space dominated by a 3:1 stretch–bend resonance zone. The EBK FFT method is found to give accurate semiclassical eigenvalues for both resonant and nonresonant states. We are unable to find a significant correlation between the resonant vs nonresonant character of a region of phase space and the failure of the approximate semiclassical procedures applied by Swamy and Hase.

The structure of the paper is as follows: The stretch–bend Hamiltonian used is described in detail in Sec. II. The spectral and EBK FFT methods are briefly reviewed in Sec. III, while results are presented in Sec. IV. Conclusions are given in Sec. V.

II. STRETCH–BEND HAMILTONIAN

The stretch–bend Hamiltonian studied in the present paper is that described in detail by Swamy and Hase,[10] and has the form

$$\begin{aligned} H =& \tfrac{1}{2} G_{rr} p_r^2 + \tfrac{1}{2} G_{\theta\theta} p_\theta^2 \\ &+ G_{r\theta} p_r p_\theta + D_r\{1 - \exp[-\beta_r (r - r_0)]\}^2 \\ &+ S(r)\left[\tfrac{1}{2} f_\theta (\theta - \theta_0)^2 + g_\theta (\theta - \theta_0)^3\right. \\ &\left. + h_\theta (\theta - \theta_0)^4\right]. \end{aligned} \tag{2.1}$$

Equation (2.1) is a two-mode model for the CH stretch (r) and HCC bend (θ) dynamics of the hydrocarbon fragment HC_2, in which the CC bond is frozen. The CH bond is taken to be a Morse oscillator, while the bending potential is expressed as a power series up to quartic in the bend displacement. Values of the various parameters appearing in Hamiltonian (2.1) are given in Table I. Note that both kinetic and potential coupling terms are present in Hamiltonian (2.1). The kinetic coupling is a consequence of the coordinate dependence of the G-matrix elements, which are[22]

TABLE I. Potential energy parameters for the Hamiltonian of Eq. (2.1).

D_r	110.60 kcal/mol
β_r	1.879 Å^{-1}
r_0	1.086 Å
f_θ	0.593 8 mdyn Å/rad^2
g_θ	−0.090 3 mdyn Å/rad^3
h_θ	0.012 0 mdyn Å/rad^4
θ_0	109.471 2°
α_1	1.531 37×10^{-7} Å^{-9}
β_1	−4.669 62 Å
α_3	2.000 00 Å^{-1}

$$G_{rr} = (m_C + m_H)/m_C m_H, \tag{2.2a}$$

$$G_{r\theta} = -\sin\theta/m_C R, \tag{2.2b}$$

$$G_{\theta\theta} = (m_C + m_H)/m_C m_H r^2 + 2/m_C R^2 - 2\cos\theta/m_C r R. \tag{2.2c}$$

Here, R is the CC bond length, which is set at its equilibrium value $R = 1.5100$ Å. Stretch–bend potential coupling occurs through the r dependence of the switching function $S(r)$, which models the attenuation of the bending force constant. Following Swamy and Hase, we consider three different functional forms for S:

$$\text{Type 1: } S(r) = 1 - \tanh[\alpha_1 (r - r_0)(r - \beta_1)^8], \tag{2.3a}$$

$$\text{Type 2: } S(r) = 1, \tag{2.3b}$$

$$\text{Type 3: } S(r) = \exp[-\alpha_3 (r - r_0)]. \tag{2.3c}$$

Type 1 is a switching function fit to *ab initio* results on CH bond dissociation in CH_4.[23] Type 2 corresponds to no potential coupling, the HCC bending force constant in this case being independent of CH stretch coordinate. Type 3 corresponds to a semiempirical BEBO[24] dependence of bending force constant on CH bond distance. Values for the parameters in Eq. (2.3) are given in Table I. Swamy and Hase found that the three different potential couplings lead to very different rates of change of bending transition energies with CH bond excitation.[10]

It should be noted that the zeroth-order frequency of the CH oscillator is approximately three times that of the harmonic HCC bend. We therefore expect a 3:1 stretch–bend resonance to be prominent in the phase space of the system. This is indeed the case, as will be seen below.

III. SEMICLASSICAL METHODS

Two semiclassical methods are applied here to determine vibrational transition energies and eigenvalues for the Hamiltonian (2.1). Both methods are based on the spectral properties of trajectories, and have been discussed in detail previously.[15–17,19–21] We briefly review each method here.

A. Mean action calculation of transition frequencies

The spectral method for approximate calculation of transition frequencies developed by Noid, Koszykowski, and Marcus[15–17] is based upon the Heisenberg correspondence principle.[18] If we have a pair of quantum states labeled by particular values of the same set of quantum numbers, and if the classical dynamics in the associated region of phase space is quasiperiodic, so that there is a direct correspondence between quantum states and invariant tori,[25] then the energy difference between states with quantum numbers $\mathbf{n}''$ and $\mathbf{n}'$ can be written approximately as

$$E(\mathbf{n}'') - E(\mathbf{n}') = \hbar\boldsymbol{\omega}\cdot\Delta\mathbf{n}, \tag{3.1}$$

where $\Delta\mathbf{n} = \mathbf{n}'' - \mathbf{n}'$, and $\boldsymbol{\omega}$ is the classical frequency vector

$$\boldsymbol{\omega} = \frac{\partial E(\mathbf{J})}{\partial \mathbf{J}} \tag{3.2}$$

evaluated at actions $\mathbf{J}$ corresponding to the mean value of the quantum numbers

$$\mathbf{n} = \tfrac{1}{2}(\mathbf{n}'' + \mathbf{n}'). \tag{3.3}$$

(Various means other than the arithmetic mean have been used, see Ref. 17.) If one of the states involved is resonant and the other is nonresonant, they are labeled by different sets of quantum numbers so that the above procedure is inapplicable.[17] The approximation (3.1) is expected to be most accurate for large quantum numbers and small $\Delta\mathbf{n}$, but has been shown to work well even at low quantum numbers for coupled oscillator systems.[15–17] The appropriate classical fundamental frequencies ω can be found by Fourier analysis of a single classical trajectory having good actions $\mathbf{J}$. If the two quantum states differ by unity in the value of a single quantum number, the transition frequency is given directly by the classical fundamental frequency of the associated mode. In practice, reasonably accurate results can be obtained by running trajectories with mean values of the *zeroth-order* actions (see Ref. 15 and Sec. IV).

B. FFT EBK Quantization of energy levels

The Fourier transform approach to semiclassical quantization has been described in detail elsewhere.[19–21,26] The method is based on the fact that, for motion in quasiperiodic regions of phase space, coordinates and momenta can be expanded as convergent Fourier series in angle variables $\boldsymbol{\theta}$[25]

$$\mathbf{q}(\boldsymbol{\theta},\mathbf{J}) = \sum_{\mathbf{k}} \mathbf{q}_{\mathbf{k}}(\mathbf{J}) e^{i\mathbf{k}\cdot\boldsymbol{\theta}}, \tag{3.4a}$$

$$\mathbf{p}(\boldsymbol{\theta},\mathbf{J}) = \sum_{\mathbf{k}} \mathbf{p}_{\mathbf{k}}(\mathbf{J}) e^{i\mathbf{k}\cdot\boldsymbol{\theta}}, \tag{3.4b}$$

where the angle variables

$$\theta_\alpha = \omega_\alpha t + \theta_\alpha^0, \quad \alpha = 1,\ldots,N, \tag{3.5}$$

and ω_α is the αth component of the fundamental frequency vector (3.2) (Fourier methods have also been used to analyze nonquasiperiodic motions.[27,28]) The action integrals

$$J_\alpha = 1/2\pi \int_0^{2\pi} d\theta_\alpha \, \mathbf{p}\cdot\left(\frac{\partial \mathbf{q}}{\partial \theta_\alpha}\right) \tag{3.6}$$

can then be expressed directly in terms of the Fourier coefficients $\{\mathbf{q}_{\mathbf{k}},\mathbf{p}_{\mathbf{k}}\}$:

$$J_\alpha = \sum ik_\alpha \, \mathbf{p}_{\mathbf{k}}^* \cdot \mathbf{q}_{\mathbf{k}}. \tag{3.7}$$

For the Hamiltonian (2.1), in which the G-matrix elements have nontrivial coordinate dependence, i.e., $\mathbf{p} \neq d\mathbf{q}/dt$, this expression for the action variables cannot be simplified further.

The result (3.7) implies that good action variables for quasiperiodic motion in nonseparable multidimensional systems can be calculated, provided accurate coordinate Fourier transforms can be found, even for systems with more than two degrees of freedom.[20] The problem of numerical determination of Fourier coefficients in a stable and accurate fashion has been solved.[20]

The result (3.7) holds for both nonresonant and resonant cases. In the absence of a commensurability between zeroth-order frequencies, assignment of the classical power spectrum is quite straightforward.[20] For resonant motion in two degrees of freedom, coordinate power spectra exhibit a characteristic form (see below), and a detailed discussion of the appropriate assignment has been given.[21] Quantization of resonant trajectories for several two-mode coupled oscillator model systems has been carried out using the FFT method.[21] In the present paper, the FFT EBK method is applied to quantize both nonresonant and 3:1 resonant states of the realistic Hamiltonian (2.1).

IV. RESULTS

A. Mean action calculation of transition frequencies

The mean action spectral method[15–17] was used to calculate frequencies for the bending transition $N_\theta = 0 \rightarrow 1$, $N_r = 0,1,2,\ldots$, for the three types of potential coupling described in Sec. II. Trajectories with mean values of the zeroth-order actions were Fourier transformed to give single quantum transition energies.

Initial conditions were chosen as follows: The CH stretch quantum number N_r was fixed at an integer value, with corresponding Morse oscillator action

$$J_r = (N_r + \tfrac{1}{2})\hbar. \tag{4.1}$$

The conjugate angle ϕ_r was chosen at random, and the associated values of the stretching coordinate r and momentum p_r calculated from the standard relation between Morse oscillator Cartesian variables and action-angle coordinates.[29] For the anharmonic bending mode, the initial bending angle θ was set for convenience at its equilibrium value θ_0, and the conjugate momentum p_θ taken to be

$$p_\theta = [2E(N_\theta)/G_{\theta\theta}(r = r_0)]^{1/2}, \tag{4.2}$$

where N_θ is the mean value of the bending quantum number for the transition $N_\theta^i \rightarrow N_\theta^f$, and $E(N_\theta)$ is a third-order polynomial in the bending quantum number N_θ obtained by a least-squares fit to the semiclassical eigenvalues of Swamy and Hase (Ref. 10, Table II):

$$E(N) = 506.0 + 1008.74N - 0.925N^2 - 0.0612N^3 \ (\mathrm{cm}^{-1}). \tag{4.3}$$

Energies for the bending transition $N_\theta = 0 \rightarrow 1$ as a function of stretching quantum number N_r obtained from quantum (open triangles), mean action spectral (filled circles),

TABLE II. $N_\theta = 0 \rightarrow 1$ transition frequencies for Types 1, 2, and 3 stretch–bend coupling (cm^{-1}).

	Type 1		Type 2		Type 3	
n_r	QM[a]	EBK[b]	QM[a]	EBK[b]	QM[a]	EBK[b]
0	995	996[NR c]	998	998[NR]	963	978[NR]
1	978	979[R d]	987	985[R]	934	943[NR]
2	953	962[NR]	971	975[NR]	904	912[NR]
3	933	933[NR]	958	965[NR]	873	871[NR]
4	913	920[NR]	947	955[NR]	842	836[NR]
5	890	899[NR]				
6	865	875[NR]				
7	842	849[NR]				

[a] Quantum mechanical variational calculation, Ref. 10.
[b] FFT EBK semiclassical calculation, this work.
[c] NR: Nonresonant trajectory.
[d] R: 3:1 resonant trajectory.

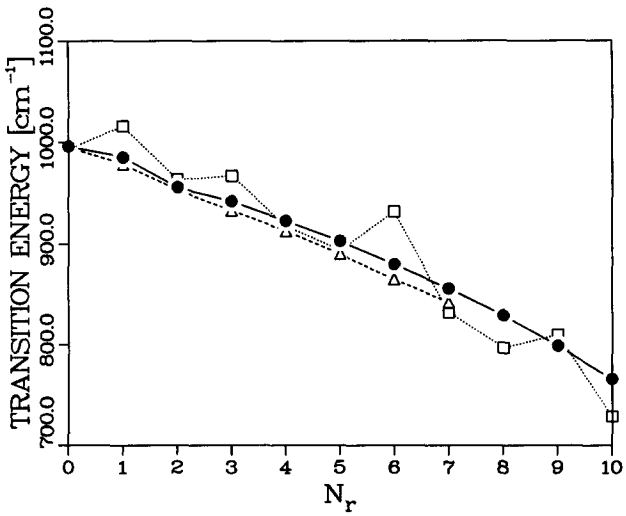

FIG. 1. Energies for the bending transition $N_\theta = 0 \rightarrow 1$ as a function of the stretching quantum number N_r for Hamiltonian (2.1) obtained from mean action spectral (filled circles, present work), quantum (open triangles, Ref. 10), and DeLeon–Heller–Miller semiclassical (open squares, Ref. 10) calculations. Type 1 stretch–bend potential coupling, cf. Eq. (2.3a).

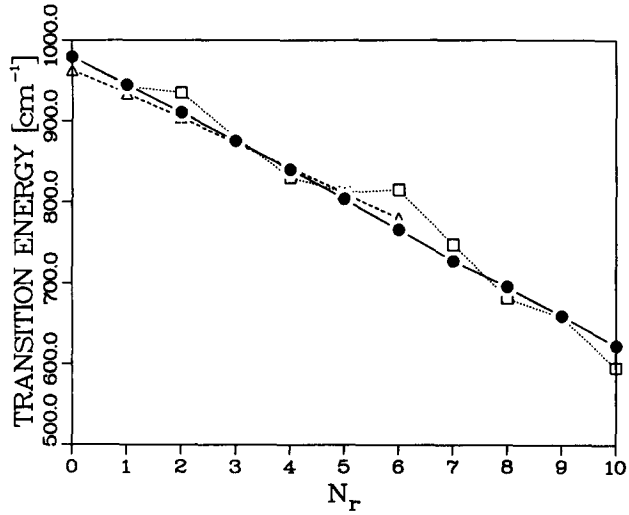

FIG. 3. As for Fig. 1, Type 3 stretch–bend potential coupling, cf. Eq. (2.3c).

and DeLeon–Heller–Miller (DHM[13–14] open squares) calculations are shown in Figs. 1–3 for Types 1, 2, and 3 couplings, respectively (cf. Figs. 1–3 of Ref. 10). The mean action spectral transition energies are in very good agreement with the variational quantum values, and are much closer than the DHM results of Ref. 10, especially for Type 2 coupling.

Swamy and Hase have suggested that stretch–bend resonances might be responsible for the poor performance of the DHM quantization method.[10] In the system studied here, the most prominent resonance is a 3:1 stretch–bend resonance, i.e., $3\omega_\theta \simeq \omega_r$. (For large values of N_r, where the CH stretch frequency is low, other stretch–bend resonances such as 8:3, 5:2, 7:3, and 2:1 appear.) In Table II, the 3:1 resonant (R) vs nonresonant (NR) character of the mean action trajectory used to calculate the transition frequency is indicated, as determined by surface of section. There is no straightforward connection between the existence of a resonant region of phase space and the failure of the DHM method to calculate accurate transition energies. Note that the accuracy of the mean action approximation is unaffected by the presence of a 3:1 stretch–bend resonance (e.g., N_θ $0 \rightarrow 1$, $N_r = 1$, Type 1 and 2 coupling). Although the coordinate power spectrum of a resonant quasiperiodic trajectory exhibits a characteristic pattern with many "sidebands" [cf. Fig. 5(c) below], the frequency of the largest, fundamental peak gives an accurate estimate of the single quantum bending transition frequency.

Transition energies for Type 2 coupling states with $N_r > 8$ are not shown in Fig. 2, as the mean action trajectories are chaotic in this region of classical phase space. In contrast to Swamy and Hase,[10] we have found chaotic trajectories for Hamiltonian (2.1) for all three types of coupling. The chaotic motion is particularly extensive for Type 2 coupling, where there is no stretch–bend potential coupling. Thus, most trajectories with $N_r + N_\theta \geqslant 12$ are found to be chaotic with Type 2 coupling (as judged by the appearance of the configuration space trajectory). Chaos in the presence of stretch–bend potential coupling (Types 1 and 3) is confined to higher energies. The suppression of global chaotic behavior by stretch–bend potential coupling is consistent with the conclusion[9] that potential coupling cancels the kinetic coupling to a certain extent, reducing the rate of stretch–bend energy transfer.

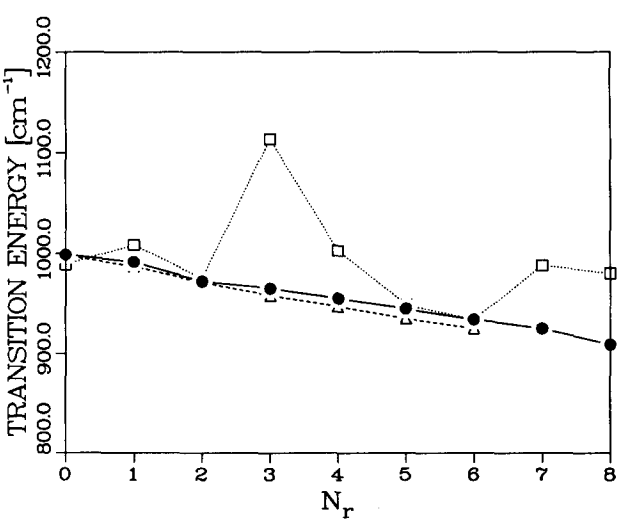

FIG. 2. As for Fig. 1, Type 2 stretch–bend potential coupling, cf. Eq. (2.3b).

B. FFT EBK quantization of energy levels

We have applied the FFT EBK semiclassical quantization method[19–21] to calculate stretch–bend vibration levels for the Hamiltonian (2.1). This method requires trajectories to be quasiperiodic, but can be used to calculate vibrational eigenvalues corresponding to both nonresonant and resonant motions.[20,21]

EBK FFT vibrational energies for potential coupling of Types 1, 2, and 3 are given in Tables III, IV, and V, respectively, together with semiclassical and quantum variational

TABLE III. Quantum and semiclassical eigenvalues for Type 1 stretch–bend coupling (cm^{-1}).

$3n_r + n_\theta$	(n_1,n_2)	(n_r,n_θ)	QM[a]	FFT[b]	SH[c]	DHM[d]
0		(0,0)	2 053	2 058	2 061	2 061
1		(0,1)	3 048	3 054	3 054	3 054
2		(0,2)	4 034	4 040	4 039	4 044
3		(0,3)	5 012	5 017	5 017	5 016
	(3, − 0)	(1,0)[e]	5 064	5 081[f]	5 060	5 058
4		(0,4)	5 981	5 986	5 981	5 988
	(4, − 0)	(1,1)[e]	6 042	6 041[f]	6 063	6 074
5		(0,5)	6 941	6 945	6 951	6 949
	(5, − 0)	(1,2)[e]	7 012	7 015	···	7 054
6		(0,6)	7 893	7 896	7 901	7 907
	(6, − 0)	(1,3)[e]	7 977	7 979	···	8 038
		(2,0)	7 944	7 952	7 938	7 976
7	(7, − 0)	(1,4)[e]	8 936	8 938	---	9 027
		(2,1)	8 897	8 914[f]	8 902	8 939
8	(8, − 0)	(1,5)[e]	9 890	9 889	---	10 019
	(8, − 1)	(2,2)[e]	9 840	9 846[f]	9 820	9 872
9	(9, − 0)	(1,6)[e]	10 838	10 833	---	11 016
	(9, − 1)	(2,3)[e]	10 775	10 779	10 807	10 816
		(3,0)	10 699	10 706	---	10 725
10		(3,1)	11 632	11 647	···	11 692
11	(11, − 0)	(1,8)[e]	12 713	12 701	···	12 740
	(11, − 1)	(2,5)[e]	12 624	12 627	···	12 667
	(11, − 2)	(3,2)[e]	12 552	12 524[f]	12 609	12 583
12	(12, − 0)	(1,9)[e]	···	13 624	···	···
	(12, − 1)	(2,6)[e]	13 540	13 542	···	13 622
	(12, − 2)	(3,3)[e]	13 468	13 481[f]	13 510	13 656
		(4,0)	13 323	13 332	13 376	13 339
13		(4,1)	14 236	14 252	14 270	14 257
14		(4,2)	15 137	15 161	15 178	15 177
15		(4,3)	16 029	16 060	16 040	16 286
		(5,0)	15 819	15 829	···	15 846
16		(5,1)	16 709	16 728	16 752	16 740
17		(5,2)	···	17 615	17 644	17 633
18		(5,3)	···	18 490	···	18 521
		(6,0)	18 187	18 197	···	18 204
19		(6,1)	19 052	19 072	19 133	19 136
20		(6,2)	···	19 935	···	19 951
21		(6,3)	···	20 786	···	20 798
		(7,0)	20 438	20 436	···	20 460
22		(7,1)	21 280	21 285	···	21 292
23		(7,2)	···	22 122	···	22 118
24		(7,3)	···	22 947	···	22 967
		(8,0)	···	22 552	···	22 553
25		(8,1)	···	23 374	23 342	23 350
27		(9,0)	···	24 524	24 464	24 533
28		(9,1)	···	25 314	25 331	25 343
29		(9,2)	···	26 087	···	26 123
30		(9,3)	···	26 868	26 862	26 894
		(10,0)	···	26 374	26 263	26 406
31		(10,1)	···	27 160	27 144	27 135

[a] Quantum mechanical variational eigenvalues, Ref. 10.
[b] FFT EBK semiclassical eigenvalues, this work.
[c] Sorbie–Handy semiclassical eigenvalues, Ref. 10.
[d] DeLeon–Heller–Miller semiclassical eigenvalues, Ref. 10.
[e] Quantum number assignments used in Ref. 10.
[f] Extrapolated eigenvalues (see the text).

values calculated by Swamy and Hase.[10] Initial conditions for all quantizing trajectories are available from the authors on request.

There are several points to note. The FFT EBK semiclassical eigenvalues are on the whole more accurate than both the Sorbie–Handy and DHM values of Swamy and Hase,[10] especially for excited states, and are in good agreement with the quantum eigenvalues. This is not unexpected, since the Sorbie–Handy[11] and Miller[13] methods both involve dynamical approximations in addition to the semiclassical approximation itself.

Tables III–V include FFT EBK eigenvalues for both nonresonant and 3:1 resonant stretch–bend states. As a result of the near 3:1 resonance between the CH stretch and bending frequencies, vibrational levels can be grouped (at low energies, at least) into *polyads*, manifolds of near-degen-

TABLE IV. Quantum and semiclassical eigenvalues for Type 2 stretch–bend coupling (cm^{-1}).

$3n_r + n_\theta$	(n_1,n_2)	(n_r,n_θ)	QM[a]	FFT[b]	SH[c]	DHM[d]
0		(0,0)	2 054	2 059	2 070	2 069
1		(0,1)	3 052	3 057	3 059	3 058
3	(3, − 0)	(0,3)[e]	···	5 027	···	···
		(1,0)	5 068	5 075[f]	5 069	5 082
4		(0,4)	···	5 999	···	···
	(4, − 0)	(1,1)[e]	6 055	6 060[f]	6 050	6 091
6		(2,0)	7 952	7 960	7 954	8 002
7	(7, − 0)	(1,4)[e]	···	8 976	···	···
		(2,1)	8 923	8 935	8 948	8 977
9		(3,0)	10 709	10 719	10 709	10 730
10		(3,1)	11 667	11 684	···	11 844
12	(12, − 0)	(2,6)[e]	···	13 728	···	···
	(12, − 1)	(3,3)[e]	···	13 629	···	···
		(4,0)	13 339	13 351	···	13 357
13		(4,1)	14 286	14 306	···	14 360

[a] Quantum mechanical variational eigenvalues, Ref. 10.
[b] FFT EBK semiclassical eigenvalues, this work.
[c] Sorbie–Handy semiclassical eigenvalues, Ref. 10.
[d] DeLeon–Heller–Miller semiclassical eigenvalues, Ref. 10.
[e] Quantum number assignment used in Ref. 10.
[f] Extrapolated eigenvalues (see the text).

erate states with the same value of the "principal quantum number"

$$N_1 = 3N_r + N_\theta. \tag{4.4}$$

For nonresonant trajectories in a given polyad, the quantizing classical actions are

$$J_r = N_r + \tfrac{1}{2} \tag{4.5a}$$

and

$$J_\theta = N_\theta + \tfrac{1}{2}, \tag{4.5b}$$

where N_r and N_θ are integers. For 3:1 resonant trajectories, the "principal" action[21] is

$$J_1 = N_1 + 2, \tag{4.6a}$$

with N_1 given by Eq. (4.4). The second quantizing action is

$$|J_2| = N_2 + \tfrac{1}{2}, \tag{4.6b}$$

with N_2 integer.

Configuration space plots and bending coordinate power spectra for quantizing trajectories corresponding to the three states of the polyad with $N_1 = 6$ are shown in Figs. 4 and 5, respectively. A (θ,p_θ) surface of section is shown in Fig. 6 for the three quantizing trajectories, which are labeled A, B, and C in order of increasing energy. (Since the energies of the three trajectories are not identical, Fig. 6 is not strictly speaking a surface of section.) The resonant character of trajectory C is clear from Fig. 6, as is the nonresonant character of trajectories A and B. The resonant nature of trajectory C is also apparent from the configuration space plot of Fig. 4(c) and the power spectrum of Fig. 5(c). Trajectory A corresponds to quantum numbers ($N_\theta = 6$, $N_r = 0$), while trajectory B has ($N_\theta = 0$, $N_r = 2$). Peaks in the nonresonant quasiperiodic power spectra in Figs. 5(a) and 5(b) are assigned in terms of the fundamental frequencies ω_θ and ω_r. That is, the frequency Ω of every peak can be written as a linear combination of the fundamentals ω_θ,ω_r:

TABLE V. Quantum and semiclassical eigenvalues for Type 3 stretch–bend coupling (cm^{-1}).

$3n_r + n_\theta$	(n_1,n_2)	(n_r,n_θ)	QM[a]	FFT[b]	SH[c]	DHM[d]
0		(0,0)	2 046	2 052	2 058	2 058
1		(0,1)	3 009	3 030	3 029	3 032
3		(1,0)	5 050	5 054	5 078	5 055
4		(1,1)	5 984	5 997	6 038	5 998
6		(2,0)	7 926	7 927	7 912	7 922
7		(2,1)	8 830	8 834	8 877	8 857
9		(3,0)	10 675	10 673	···	10 672
10		(3,1)	11 548	11 544	···	11 552
12		(4,0)	13 295	13 290	13 306	13 321
13		(4,1)	14 137	14 126	···	14 151

[a] Quantum mechanical variational eigenvalues, Ref. 10.
[b] FFT EBK semiclassical eigenvalues, this work.
[c] Sorbie–Handy semiclassical eigenvalues, Ref. 10.
[d] DeLeon–Heller–Miller semiclassical eigenvalues, Ref. 10.

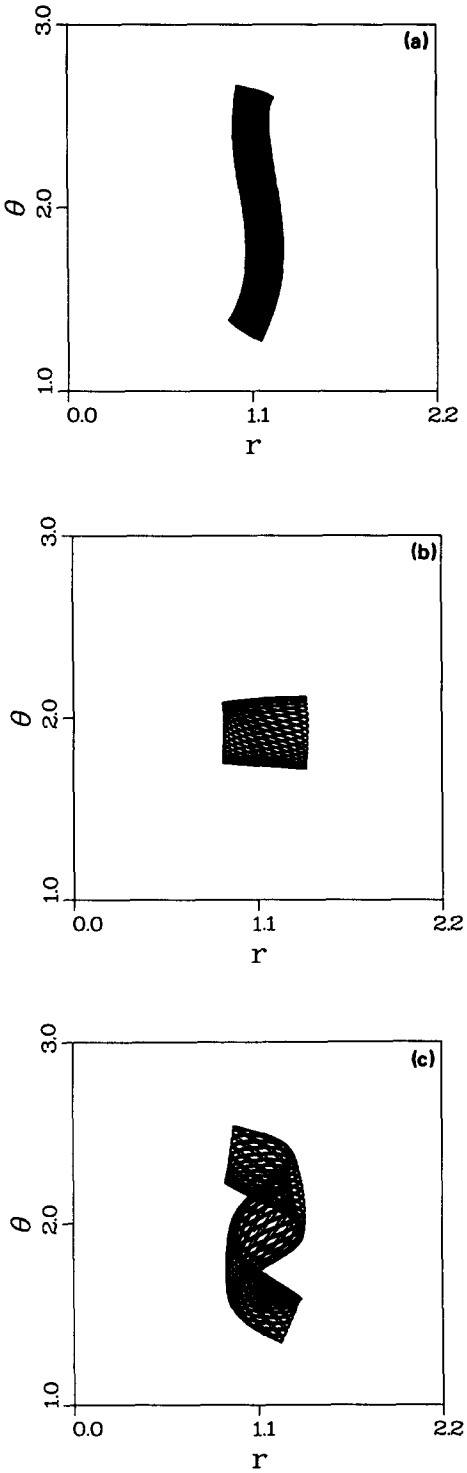

FIG. 4. Configuration space (r,θ) plots of the quantizing trajectories corresponding to the polyad of three eigenstates of Hamiltonian (2.1) with $3N_r + N_\theta = 6$. (a) $N_\theta = 6, N_r = 0$, nonresonant. (b) $N_\theta = 0, N_r = 2$, nonresonant. (c) $N_1 = 6, N_2 = 0$, resonant.

$$\Omega = k_\theta \omega_\theta + k_r \omega_r, \tag{4.7}$$

k_θ and k_r integers.

On the other hand, the power spectrum of Fig. 5(c) is most appropriately assigned in terms of the resonant frequencies $(\omega_1^r \simeq \omega_\theta \simeq \omega_r/3, \omega_2^r)$. (These frequencies correspond to the dynamical assignment of Ref. 21.) If the principal action J_1 of a 3:1 resonant trajectory is held fixed, and the

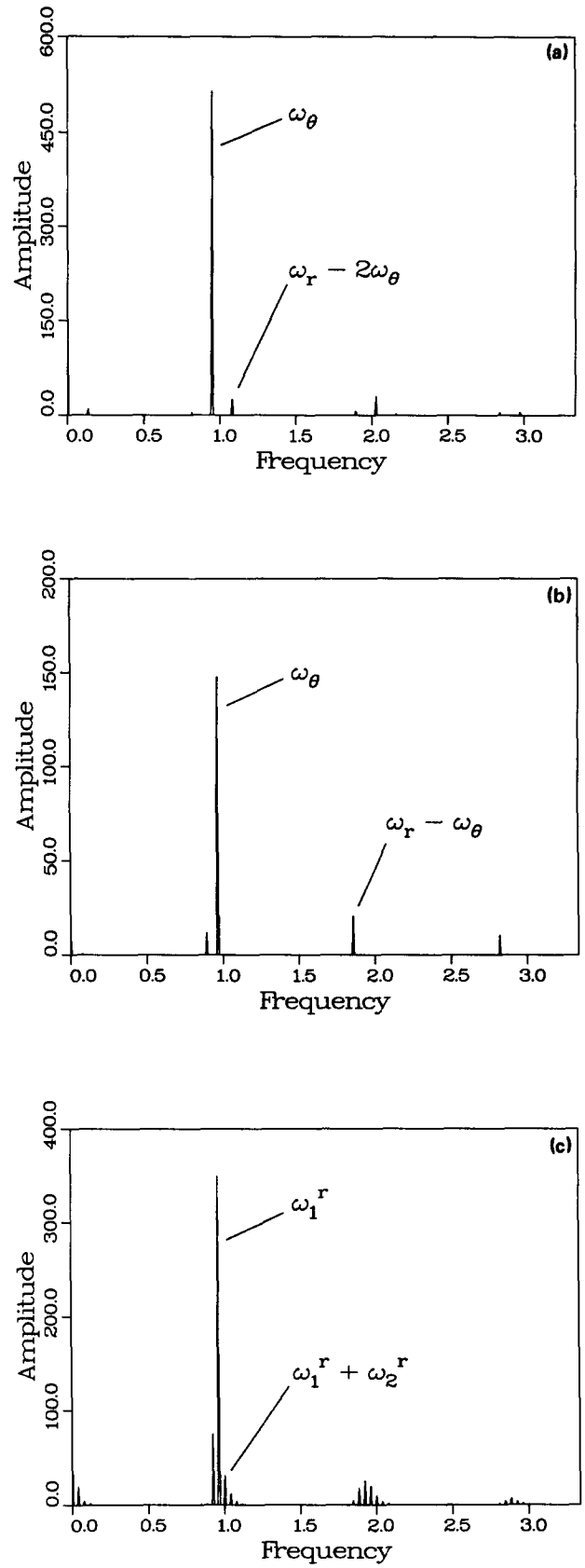

FIG. 5. Bending coordinate power spectra for the quantizing trajectories corresponding to the polyad of three eigenstates of Hamiltonian (2.1) with $3N_r + N_\theta = 6$. (a) $N_\theta = 6, N_r = 0$, nonresonant assignment of peaks. (b) $N_\theta = 0, N_r = 2$, nonresonant assignment of peaks. (c) $N_1 = 6, N_2 = 0$, resonant assignment of peaks. Frequency units are 10^3 cm^{-1}.

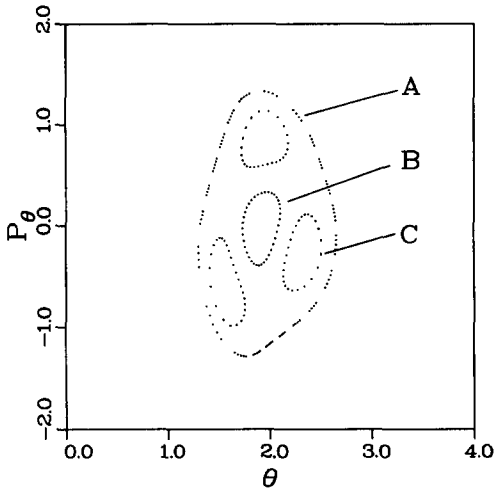

FIG. 6. (θ,p_θ) surface of section for the quantizing trajectories corresponding to the polyad of three eigenstates of Hamiltonian (2.1) with $3N_r + N_\theta = 6$. Trajectory A has $N_\theta = 6, N_r = 0$, trajectory B has $N_\theta = 0, N_r = 2$, and trajectory C has $N_1 = 6, N_2 = 0$.

magnitude of the second action $|J_2|$ increased (corresponding to increasing the areas of the resonant islands in Fig. 6), the energy of the trajectory is found to decrease, i.e., $\partial E / \partial |J_2| < 0$. If the action J_2 is defined to be positive, the classical resonant frequency ω_2' must therefore be negative. Conversely, fixing ω_2' to be positive leads to the action J_2 being negative. A similar phenomenon was noted in Ref. 21; the R-type 2:1 resonant trajectories discussed in Sec. III E of Ref. 21 have negative actions J_2 when ω_2 is defined to be positive [cf. Fig. 11(a) of Ref. 21]. The resonant trajectory C corresponds to quantum numbers $N_1 = 6, N_2 = 0$.

In some cases, the quantizing trajectory lies near the separatrix[30] dividing resonant from nonresonant motion. Calculation of actions using the Fourier method then becomes difficult due to overlap of spectral peaks as the frequency ω_2' tends to zero at the separatrix. In addition, iteration of initial conditions to determine quantizing trajectories near the separatrix can lead to the updated trajectory changing character from resonant to nonresonant or vice versa. For certain states, trajectories satisfying primitive EBK quantization conditions, either resonant or nonresonant, do not exist.[21] For all these cases, quantizing energies are approximated by linear extrapolation from a nearby nonquantizing trajectory.[14] Energy levels obtained in this fashion are identified in Tables III–V.

Single quantum bending transition energies calculated from EBK FFT vibrational eigenvalues are very close to the quantum values of Ref. 10 (see Table II), and are not plotted in Figs. 1–3. The root-mean-square deviations of the $N_\theta = 0 \rightarrow 1$ transition energies from the quantum values are 4 (Type 1), 4 (Type 2), and 8 cm^{-1} (Type 3).

V. CONCLUSIONS

In this paper we have applied semiclassical methods to determine vibrational eigenvalues and transition frequencies for the HC_2 fragment recently studied by Swamy and Hase.[10] It has been shown that the FFT EBK approach,[19–21] which is an exact primitive semiclassical method, yields accurate stretch–bend energies for the realistic HC_2 Hamiltonian considered, both for nonresonant and for 3:1 resonant states. Since the FFT EBK method can be applied to systems with more than two degrees of freedom,[20] these results are encouraging for future applications to chemically interesting systems. The approximate mean action spectral method due to Noid, Koszykowski, and Marcus[15] has been found to lead to remarkably accurate estimates for bending transition energies, even in cases where the mean action trajectory is resonant. These results contrast with the relatively poor accuracy obtained by Swamy and Hase using the Miller extrapolation approximation.[13]

Miller's approximate method is of course easier to implement than exact quantization procedures such as the FFT EBK method, and it is therefore unfortunate that the method performs badly for the problem under discussion.[10] One motivation for the present work was to investigate whether the existence of stretch–bend resonances was responsible for the poor results obtained with Miller's method, as suggested by Swamy and Hase.[10] Our analysis shows that this is not the case. Although we have demonstrated that appreciable regions of phase space are associated with a 3:1 stretch–bend resonance, there appears to be no correlation between the presence or absence of resonant motions and the poor performance of the DeLeon–Heller–Miller method.

Stretch–bend potential coupling has important spectral and dynamical consequences in the particular Hamiltonian under study,[10] and in other CH local mode containing systems.[7] Chaotic trajectories have been found for all three types of potential coupling considered here, with the stretch–bend coupling tending to suppress the appearance of chaos. Elsewhere,[9] we have studied the effects of stretch–bend potential coupling on the stability of the periodic orbit[8] corresponding to CH stretching motion in a two-mode model system, and have shown that the range of stability can be correlated with trends in CH overtone relaxation rates found in full scale trajectory calculations on planar benzene.[7]

ACKNOWLEDGMENTS

This work was supported by NSF Grant No. CHE-8410685, and by the US–Spain Cooperative Program in Basic Sciences. Computations reported here were performed in part on the Cornell National Supercomputer Facility, which is supported in part by the NSF and IBM Corporation. C. C. M. acknowledges support of the U. S. Army Research Office, through the Mathematical Sciences Institute of Cornell University. G. S. E. acknowledges partial support of the Alfred P. Sloan Foundation.

[1] T. Uzer, Chem. Phys. Lett. **110**, 356 (1984).
[2] G. A. Voth and R. A. Marcus, J. Chem. Phys. **82**, 4064 (1985).
[3] E. L. Sibert III, W. P. Reinhardt, and J. T. Hynes, J. Chem. Phys. **81**, 1115 (1984); E. L. Sibert III, J. T. Hynes, and W. P. Reinhardt, *ibid.* **81**, 1135 (1984).
[4] G. A. Voth, R. A. Marcus, and A. H. Zewail, J. Chem. Phys. **81**, 5494 (1984).
[5] K. V. Reddy, D. F. Heller, and M. J. Berry, J. Chem. Phys. **76**, 2814 (1982).
[6] R. J. Wolf, D. S. Bhatia, and W. L. Hase, Chem. Phys. Lett. **132**, 493 (1986), and references therein.

[7]D.-H. Lu, W. L. Hase, and R. J. Wolf, J. Chem. Phys. **85**, 4422 (1986); D.-H. Lu and W. L. Hase, report (unpublished).
[8]E. J. Heller, E. B. Stechel, and M. J. Davis, J. Chem. Phys. **73**, 4720 (1980).
[9]A. Garcia-Ayllon, J. Santamaria, and G. S. Ezra (in preparation).
[10]K. N. Swamy and W. L. Hase, J. Chem. Phys. **84**, 361 (1986).
[11]K. S. Sorbie, Mol. Phys. **32**, 1577 (1976); K. S. Sorbie and N. C. Handy *ibid.* **32**, 1327 (1976); **33**, 1319 (1977).
[12]D. W. Noid and R. A. Marcus, J. Chem. Phys. **67**, 559 (1977), Ref. 26.
[13]W. H. Miller, J. Chem. Phys. **81**, 3573 (1984).
[14]N. De Leon and E. J. Heller, J. Chem. Phys. **78**, 4005 (1983).
[15]D. W. Noid, M. L. Koszykowski, and R. A. Marcus, J. Chem. Phys. **67**, 404 (1977).
[16]M. L. Koszykowski, D. W. Noid, and R. A. Marcus, J. Phys. Chem. **86**, 2113 (1982).
[17]D. M. Wardlaw, D. W. Noid, and R. A. Marcus, J. Phys. Chem. **88**, 536 (1984).
[18]W. Heisenberg, *The Physical Principles of the Quantum Theory* (Dover, New York, 1949).
[19]C. W. Eaker, G. C. Schatz, N. De Leon, and E. J. Heller, J. Chem. Phys. **81**, 5913 (1984).
[20]C. C. Martens and G. S. Ezra, J. Chem. Phys. **83**, 2990 (1985).
[21]C. C. Martens and G. S. Ezra, J. Chem. Phys. **86**, 279 (1987).
[22]E. B. Wilson, Jr., J. C. Decius, and P. C. Cross, *Molecular Vibrations* (Dover, New York, 1980).
[23]R. J. Duchovic, W. L. Hase, and H. B. Schlegel, J. Phys. Chem. **88**, 1339 (1984).
[24]H. S. Johnson, *Gas Phase Reaction Rate Theory* (Ronald, New York, 1966).
[25]I. C. Percival, Adv. Chem. Phys. **36**, 1 (1977).
[26]C. W. Eaker and G. C. Schatz, J. Chem. Phys. **81**, 2394 (1984); R. J. Duchovic and G. C. Schatz, *ibid.* **84**, 2239 (1986).
[27]J. D. McDonald and R. A. Marcus, J. Chem. Phys. **65**, 2180 (1976).
[28]C. C. Martens, M. J. Davis, and G. S. Ezra, Chem. Phys. Lett. (submitted).
[29]C. C. Rankin and W. H. Miller, J. Chem. Phys. **55**, 3150 (1971).
[30]A. J. Lichtenberg and M. A. Lieberman, *Regular and Stochastic Motion* (Springer, New York, 1983).